

True ternary fission of $^{252}\text{Cf}(\text{sf})$, the collinear decay into fragments of similar size

This content has been downloaded from IOPscience. Please scroll down to see the full text.

2014 J. Phys.: Conf. Ser. 569 012040

(<http://iopscience.iop.org/1742-6596/569/1/012040>)

View [the table of contents for this issue](#), or go to the [journal homepage](#) for more

Download details:

IP Address: 131.169.4.70

This content was downloaded on 14/01/2016 at 09:10

Please note that [terms and conditions apply](#).

True ternary fission of $^{252}\text{Cf}(\text{sf})$, the collinear decay into fragments of similar size

W von Oertzen^{1,2} and A K Nasirov²

¹ Helmholtz-Zentrum Berlin, 14109 Berlin, Germany

² Joint Institute for Nuclear Research, Dubna, Russia

E-mail: oertzen@helmholtz-berlin.de

Abstract. The ternary decay in $^{252}\text{Cf}(\text{sf},\text{fff})$, with three cluster fragments of different masses (e.g. ^{132}Sn , $^{52-48}\text{Ca}$, $^{68-72}\text{Ni}$), has been observed by the FOBOS group in JINR. This work has established a new decay mode of heavy nuclei, the collinear cluster tripartition, (CCT). This “true ternary fission” of heavy nuclei has been predicted many times in theoretical works during the last decades. In the present report we discuss true ternary fission (FFF) into three nuclei of almost equal size (e.g. $Z=98 \rightarrow Z_i = 32, 34, 32$) and other fission modes in the same system. The possible fission channels for $^{252}\text{Cf}(\text{sf})$ are predicted from potential-energy (PES) calculations. These PES's show pronounced minima for several ternary fragmentation decays, suggesting a variety of collinear ternary fission modes. The FFF-decays have very similar dynamical features as the previously observed collinear CCT-decays, the central fragment has *very small* kinetic energy. The data of the cited experiment allow the extraction of the yield for some FFF-decays, by using specific gates on the measured parameters.

1. Introduction

Binary fission has been studied intensively over the last decades, for an overview there is the book edited by C. Wagemans: The Nuclear Fission Process [1], covering all important aspects of this process. The term ternary fission, has been used for light particle accompanied binary fission. For such decays, when a third light particle is emitted *perpendicular* to the binary fission axis compilations are available [2]. These must be considered to be emitted from an oblate configuration, the corresponding yields decrease strongly as function of increasing mass(charge) of the third particle [2]. Recent experimental observations and numerous theoretical predictions [3, 4, 5] suggest, however, that in heavy systems and for ternary fragments with larger charge, ternary *collinear* decay from a prolate configuration is preferred. The various ternary decay modes studied here, are in a collinear geometry and are now referred to as “true ternary fission”, see also e.g. Zagrebaev *et al.* in ref. [6]. More recent surveys of clustering effects in fission and other binary decays can be found in recent articles by G. Adamian, N. Antonenko and W. Scheid [7], and by D. Poenaru and W. Greiner [8]. Quite important for the discussion of the relative probabilities of oblate to prolate ternary fission is the experiment by Schall *et al.* [9], performed to detect ternary fission from an oblate configuration with three heavier fragments using several detectors covering large (90°) angles each to detect a *triangular shape of the decay-vectors*. This experiment gave a negative result, with an upper limit of the probability for this decay of $1.0 \cdot 10^{-8}/(\text{binary fission})$.



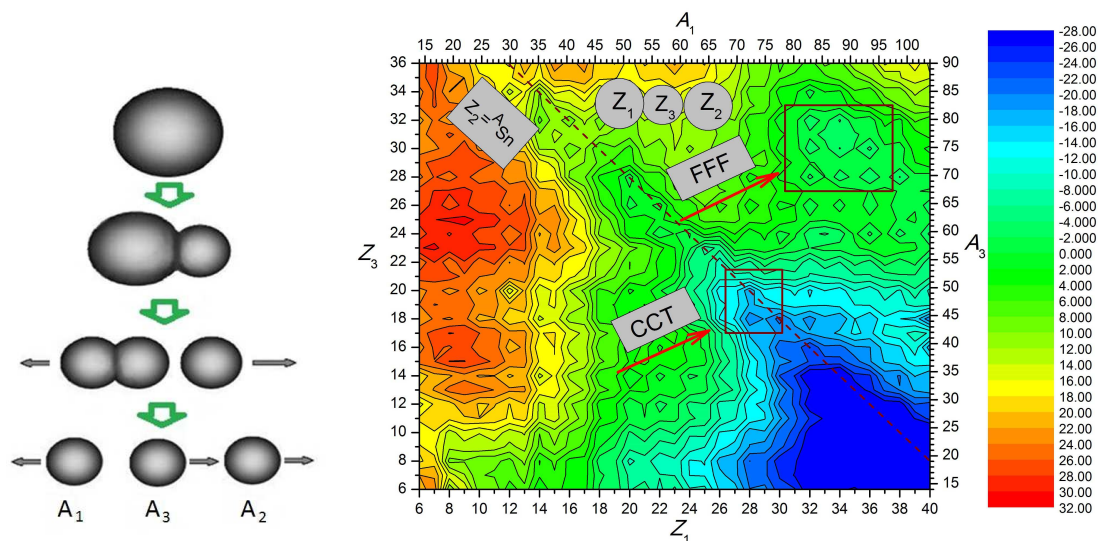


Figure 1. Left side: Schematic illustration of sequential collinear ternary fission into fragments of comparable mass. Right side: Contour plot of the PES as function of two parameters, Z_1 , Z_3 , showing the preference of the arrangement with $Z = 20$ at the center: (Ni, Ca, Sn).

2. Ternary collinear decays

Ternary fission into fragments with comparable masses is a process, which occurs in heavy nuclei under conditions of large values of the fissility parameter: X , for the ratios $Z^2/A > 31$. The decay into three heavier fragments (true ternary fission) is found to be collinear, as in fact often predicted in the last decades [3, 4, 5]. Recent experiments of two fragment coincidences with two FOBOS-detectors [10] placed at 180° , using the missing mass approach, have established the phenomenon of *collinear cluster tripartition*, the CCT-decay, for the spontaneous decay of $^{252}\text{Cf}(\text{sf},\text{fff})$. A similar ternary fission mode has been observed for neutron induced fission in $^{235}\text{U}(\text{n}_{\text{th}},\text{fff})$, see refs. [10, 11, 12]. In this fission mode, the CCT, typical fragments are isotopes (clusters, nuclei with closed shells) of Sn, Ni, and Ca. The latter, Ca, as the smallest third particle is positioned along the line connecting Sn and Ni, in this way minimizing the potential energy. This is illustrated in Fig. 2.

In the experiments described in refs. [10, 11], two of the three fragments, moving towards one of the detectors (called arm1) are dispersed in angle in the source backing. It is assumed that due to this small angular dispersion one of the fragments is lost in arm1 on a structure in front of the detectors. Thus binary coincidences are obtained with the missing mass method (A_3 , missing Ca isotopes). This new exotic decay can be understood as the breakup of very (prolate deformed) elongated hyper-deformed shapes, as discussed for hyper-deformation in ^{236}U in ref. [13]. The decay is considered with two sequential neck ruptures [12, 14], as illustrated in Fig.1. Actually the central fragment A_3 has extremely low energy (see Fig.5) and is mostly lost.

The main experimental effect in the missing mass method in the binary coincidences is the difference in the counting rates (mass spectra) in the two arms of the coincidence arrangement: Only in one arm1 (see ref. [10]) two fragments of the ternary decay travel through the dispersive media, the source backing and the foils of the start detector. Thus the dispersive effect (angular dispersion of $1\text{-}2^\circ$) of the two fragments from the ternary decay, is only present in arm1! Thus the missing mass effect appears in the counting rate difference of the mass spectra of arm1 and arm2 (as the difference $N(\text{arm1})-N(\text{arm2})$).

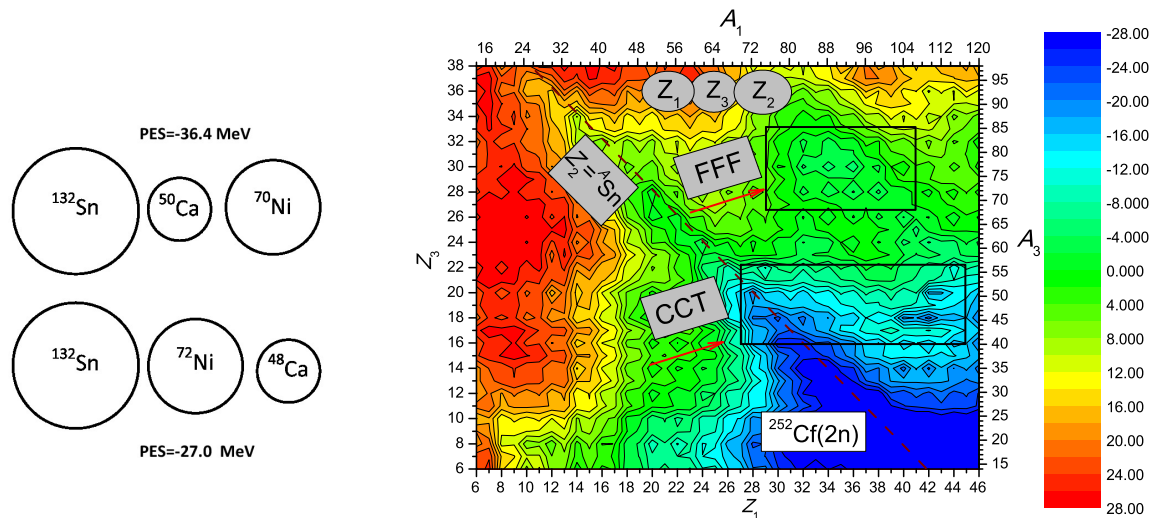


Figure 2. Schematic illustration of the Coulomb energy in ternary fission of ^{252}Cf into three cluster fragments, with isotopes of Sn, Ca and Ni. Right side: The contour map of the potential energies surface (PES) for decays with three nuclei in an arrangement, as indicated in the figure. The PES is shown as function of two parameters Z_1 and Z_3 , with the possible variations of the charges and masses of the decay products with values of (A_i/Z_j) , for A_3 from 16 - 100 and for A_1 from 18 - 120. This PES has a larger scale, showing the FFF-cases with three fragments of $Z = (32, 34, 32)$ and other cases with $Z_3 = 18$ at the center and $Z_{1,2} = (40, 42)$.

3. Potential energy surfaces

The fission processes is considered to be a statistical decay of the total (compound) nucleus, CN, as already discussed in 1939 by N. Bohr and J.A. Wheeler [15]. Actually the ternary decay occurs with two neck ruptures in a short time-sequence, each of the ruptures being governed by the internal barriers and the potential energies surface (PES) in each configuration, as also discussed in ref. [16]. The PES are obtained as described in ref. [17]. The total *phase space* of these statistical decays is determined by:

- i) the energy balance and thus the details of the *potential energy surface*, PES, namely, its valleys and hills,
- iii) the internal barriers for the two necks,
- iv) the Q_{GGG} -values, the latter determining the kinetic energies and the number of possible fragment (isotope) combinations,
- v) the excitation energy range in the individual fragments,
- vi) the momentum range,
- vii) the number of excited states (or the density of states) in each of the fragments, the combinations consisting of 2(3) isotopes, and by
- viii) the spin (J) multiplicity in these excited states with spins up to $(6-8)^+$ (phase space factor $(2J + 1)$).

For the ternary decays of ^{252}Cf , the PES's, the contour-plot in Fig.2 shows distinct minima for various charge combinations with $\Sigma_Z = 98$:

- i) for CCT $Z_3 = 20$, and $Z_1 = 28$, this is the main CCT-mode in refs. [10] and
- ii) less pronounced for $Z_3 = 28$, and $Z_1 = 20$, as observed in ref. [10, 11]. The complementary fragments with Z_2 are isotopes of Sn ($Z = 50$). The PES shows a pronounced valley with charge $Z_2 = 50$, with the closed shell for the number of protons, because of the dominance of the Coulomb interaction, the proton shells are most important. In addition we observe a

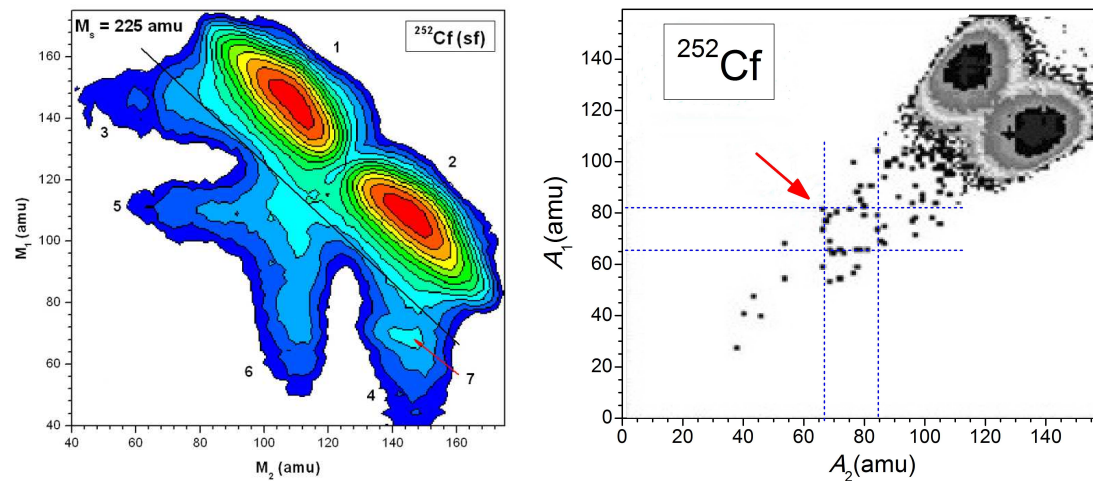


Figure 3. Left side: Binary coincidences of fragments in the spontaneous decay of $^{252}\text{Cf}(\text{sf})$ from the inclusive data measured in ref. [10], the outer fragments (A_1, A_2, M_1, M_2) are registered. Right side: For the selection of FFF decays, a gate with the condition for velocities and momenta, ($V_1 \approx V_2$, and $P_1 \approx P_2$) is chosen. Remnants of the binary fragments in coincidences are seen. The region of the FFF-decays is marked. Missing fragments (A_3), here are isotopes of nuclei with ($Z_3 = 30 - 36$). Points above this region are true coincidences of other symmetric ternary decays, from ref.[18].

pronounced region of minima for the symmetric charge combinations with three comparable fragments, for the FFF-decays (this decay is marked as FFF):

iii) ($Z_1 = 32, 34, 32$), $Z_3 = (34, 32, 30)$, the fragment Z_2 has an equivalent role as the other two and Z -values $Z_2 = 32, 34$, occur - we have an almost symmetric ternary decay. Because of this fact, permutations of the labels including Z_2 in the figure of the PES (contour plots in Fig.2) will produce similar results, and a symmetric shape of the coincident events. This is suggested by the rectangular two-dimensional field of the binary coincident events in the favored region (obtained by the reflection of the labels) in Fig. 3.

4. Experimental observations

In the original observation of CCT a wide region of missing fragment masses has been observed, which is manifested as a wide bump in the difference of the counting rates between arm1 and arm2. The yield contains many ternary mass combinations, seen as a large background in this mass region (see in the left side of Fig.3). For the symmetric decay we have to remove the background in the middle mass region. In these experimental data, we have the possibility to select events with the conditions on comparable values of the velocities $V_3 \approx V_2$ and $V_3 \approx V_1$, defining a symmetric decay, see Fig. 3, right side. This choice reduces completely the background due to the scattering tails seen in the inclusive experimental data. This background dominates the inclusive original data shown in the Fig. 3, left side, from ref. [10]. In the experiment the masses and velocities of the fragments are obtained by measurements of time of flight and energy. Because of the symmetry discussed before, the events appear in a rectangular region (for A_1, A_2) in the ranges of masses for all three fragments: (64 – 84) and (64 – 82). This corresponds to the true ternary fission into three equivalent fragments, (FFF) in ref. [18], as predicted by the PES's, Fig. 2.

As a surprise we observe in the PES for ^{252}Cf another region for FFF decays, they are suggested by the minima in the region of charges with $Z_1 = 40 - 42$, combined with values of $Z_3 = 18$, which for Cf ($Z = 98$) has to be complemented by a fragment with charges $Z_2 =$

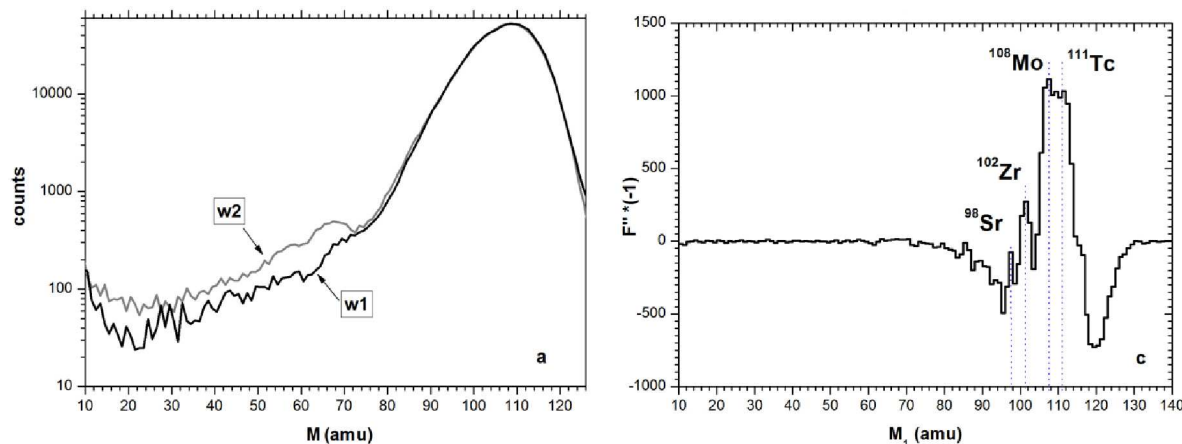


Figure 4. Extraction of the yield of the “Mo-Ar”-mode [22]. The mass spectra, the data are projected to the A_1 axis for arm1 and arm2, left side, measured in ref. [10] for binary coincidences. Right side: the derivative of the difference of the the two spectra, events in the region of ^{106}Mo appear. Missing fragments, (A_3), here are isotopes of Ar with ($Z_3 = 18$).

40. This is again a rather symmetric decay. The dominating effect comes from the closed shell properties of the central smaller fragment with $Z_3 = 18$ and masses $A_3 = 44-46$, which appears as a closed neutron shell with $N = 28$ (^{46}Ar). Actually the isotope ^{46}Ar shows strong closed shell effects with a 2^+ -state at 1.554 MeV as described in ref.[19]. Also the properties of the *Mo-isotopes* are remarkable, see recent references in ref.[20]. In a binary coincidence study the formation of the pair ($^{106}\text{Mo}+^{144}\text{Ba}$, two neutrons missing) has the highest yield. There is a sharp transition from spherical to prolate deformation in the region of $A = 102$ (spherical) to $A = 106$ (deformed with $Q = 5$ barn). Quite important we note, that the favored region with $Z_3 = 18$, corresponding to (^{46}Ar) appears also as a valley in the PES for ^{236}U , $\text{U}(Z = 92)$. Now the complementary charges are $Z_1 = 34, 36$ and $Z_2 = 40$. This case is not as symmetric as the previous one, the persistence of the strong binding in the lighter fragment points to the fact, that the valley of the binding energy as function of N and Z forms a steeper parabola for lighter nuclei, compared to the more shallow valley of the binding energies in heavier nuclei.

Inspecting the PES in Fig. 2 there are other ternary decay modes suggested by minima of the potential energies, with e.g. larger values of the masses/charges of the fragments at the two borders of the total (prolate) nucleus. In addition there are deep valleys, particularly for smaller central fragments, for A_3 , such as $A_3 = ^{22}\text{Ne}(Z_3 = 10)$, $^{18-20}\text{O}(Z_3 = 8)$, as well as for C-isotopes, see ref. [18].

In order to extract the yield of the FFF-mode with the (^{46}Ar) as the central fragment, we need a presentation of the data without background. We use as previously the difference between the counting-rates between arm1 and arm2, in the region of interest (Fig.3). As suggested by Kamanin and Pyatkov [22] we can obtain the counting rate for this specific ternary channel covered by the background in the inclusive data. In arm1 the CCT-events are removed from the smooth region, and they appear at a lower mass value of the missing mass, the complement to $[A_1 - A_3]$. The complement (the missing mass) is stopped at the entrance grid of the ionization chamber. This extra counting rate can be made visible by taking the derivative in the spectra of $N(\text{arm1}-\text{arm2})$ (right side in Fig.4). A rather strong peak appears in the mass region of $A_2 = (^{106}\text{Mo} - ^{110}\text{Tc})$.

A final remark on the possibility of triple coincidences. It has often been asked to make experiments, where all three fragments are registered. The kinematics of the process has been studied by Vijayaraghavan *et al.* [14] using the assumption of a sequential decay process. The

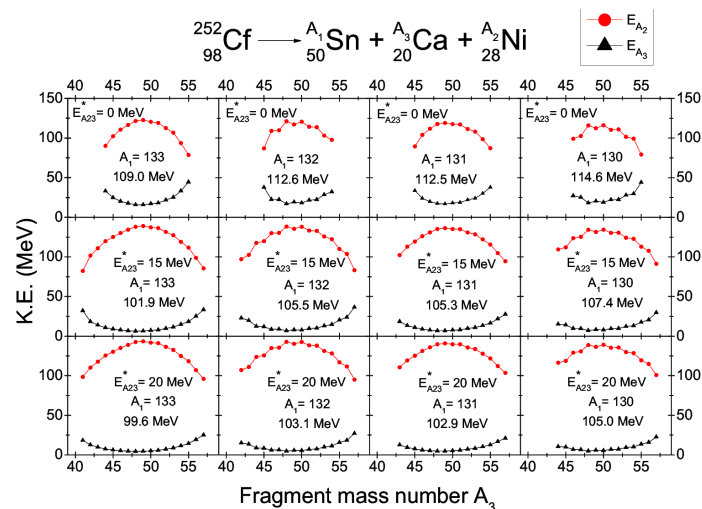


Figure 5. Kinetic energies of fragments in the sequential decay $A \rightarrow (A_1 + A_{23}), A_{23}(\text{Ex}) \rightarrow A_3 + A_2$ as obtained in ref. [14]. The kinetic energies of A_2 and A_3 are shown. With different excitation energies in A_{23} of 0.0, 15 MeV and 30 MeV. For only 10 MeV the kinetic energy of A_3 is very small and A_3 can not be detected (figure from ref.[14]).

kinetic energies of all three fragments are obtained, they are shown in Fig.5. as function of increasing excitation energy of the intermediate fragment A_{23} , which is needed for a sizeable probability of fission. The kinetic energy of A_3 becomes very small. Actually it can be expected for most (fff) experiments, that A_3 is absorbed in the target and the target backing.

References

- [1] Wagemans C (ed) 1991 *The nuclear fission process*, (CRC Press Inc., Boca Raton, Florida USA)
- [2] Gönnerwein F 2004 *Nucl. Phys. A* **734** 213
- [3] Diehl D, Greiner W 1974 *Nucl. Phys. A* **229** 29
- [4] Poenaru D N, Gherghescu R A and Greiner W 2005 *Nucl. Phys. A* **747** 182
- [5] Manimaran K *et al.* 2011 *Phys. Rev. C* **83** 034609
- [6] Zagrebaev V I, Karpov A V and Greiner W 2010 *Phys. Rev. C* **81**, 044608 also Zagrebaev V I and Greiner W 2010 in *Lecture Notes in Physics* **818** 267-315 *Clusters in Nuclei*, Vol. 1 Beck C (ed.), Chapter 7, Springer-Verlag (Heidelberg, Berlin)
- [7] Adamian G, Antonenko N and Scheid W 2012 in *Lecture Notes in Physics* **848** 165-228 *Clusters in Nuclei*, Vol.2, Beck C (ed), Springer-Verlag Berlin Heidelberg 2012.
- [8] Poenaru D and Greiner W 2010 in *Lecture Notes in Physics* **875** 1-56 *Clusters in Nuclei*, Vol.1, Beck C (ed), Springer-Verlag Berlin Heidelberg
- [9] Schall P *et al.* 1987 *Phys. Lett. B* **191** 339
- [10] Pyatkov Yu V *et al.* 2010 *Eur. Phys. J. A* **45** 29
- [11] Pyatkov Yu V *et al.* 2012 *Eur. Phys. J. A* **48** 94
- [12] von Oertzen W, Pyatkov Y V and Kamanin D 2013 *Acta Phys. Polonica* **44** 447 Zakopane Conference
- [13] Csatlos M, Krasnahorkay A, Thirof P G, *et al.* 2005 *Phys. Letters B* **615** 213
- [14] Vijayaraghavan K R, von Oertzen W and Balasubramaniam M 2012 *Eur. Phys. J. A* **48** 27
- [15] Bohr N and Wheeler J A 1939 *Phys. Rev.* **56** 426
- [16] Tashkodajev R B, Nasirov A K and Scheid W 2011 *Eur. Phys. J. A.* **47** 136
- [17] Nasirov A K *et al.* 2014 *Phys. Scripta* **89**, 054022 (2014).
- [18] von Oertzen W and Nasirov A K 2014 *Phys. Letters B* **734**, 234
- [19] Fornal B, Broda R, Krolas R W 2000 *et al. Eur. Phys. J. A* **7**, 147
- [20] Roddriguez R *et al.* 2010 *Phys. Letters B* **691** 202
- [21] Mukhopadhyay S *et al.* 2012 *Phys. Rev. C* **85** 064321
- [22] Kamanin D and Pyatkov Y V 2014 in *Lecture Notes in Physics* Vol. **875** 183-246 *Clusters in Nuclei*, Vol.3 Beck C (ed), Chapter 6. Springer(Heidelberg, Berlin)